

# Complex Empirical Mode Decomposition for Multichannel Information Fusion

Danilo P. Mandic<sup>1</sup>, George Souretis<sup>1</sup>, Wai Yie Leong<sup>1</sup>, David Looney<sup>1</sup>, Marc M. Van Hulle<sup>2</sup>, and Toshihisa Tanaka<sup>3</sup>

Imperial College London, UK<sup>1</sup>, KU Leuven, Belgium<sup>2</sup>, and Tokyo University of Agriculture and Technology, Japan<sup>3</sup>

Information “fusion” via signal “fission” is addressed in the framework of Empirical Mode Decomposition (EMD). In this way, a general nonlinear and non stationary signal is first decomposed into its oscillatory components (fission); the components of interest are then combined in an ad hoc or automated fashion in order to provide greater knowledge about a process in hand (fusion). The extension to the field of complex numbers  $\mathbb{C}$  is particularly important for the analysis of phase-dependent processes, such as those coming from sensor arrays. This allows us to combine the data driven nature of EMD with the power of complex algebra to model amplitude-phase relationships within multichannel data. The analysis shows that the extensions of EMD to  $\mathbb{C}$  are not straightforward and that they critically depend on the criterion for finding local extrema within a complex signal. For rigour, convergence of EMD is addressed within the framework of fixed point theory. Simulation examples on information fusion for brain computer interface (BCI) support the analysis.

## 1.1 Introduction

Signals obtained by standard data acquisition techniques are real-valued and naturally, the processing of such signals is performed in the field of real numbers  $\mathbb{R}$  (or  $\mathbb{R}^n$  for multichannel recordings). Notice however that a complex representation of a real signal can be both intuitive and useful, since this way both the amplitude and phase relationships between the data streams can be modelled simultaneously. Additionally, several important signal processing areas (telecommunications, sonar, radar, to mention but a few) use complex-valued data structures.

For single channel signal analysis, Fourier Spectral theory is the best established tool for the complex (frequency) domain processing of linear and stationary signals. Since real world signals are typically non stationary (and nonlinear), for which Fourier analysis is not well suited, we need to resort to time frequency analysis techniques such as the Short Time Fourier Transform

(STFT) and Wavelet Transform (WT). Despite the power of these techniques, they still rely on some kind of projection on a set of pre-defined bases; this makes some areas of their application, particularly when focusing on high frequency content, rather limited [7]. An alternative approach is Empirical Mode Decomposition (EMD) [7], a data driven time-frequency analysis technique that has an enormous appeal for nonlinear, non-stationary signals.

### 1.1.1 Data Fusion Principles

Knowledge extraction and data fusion are at the very core of modern technology, their principles have been long studied in various areas of information theory, signal processing and computing [5, 12, 16, 17]. A recent overview of data and sensor fusion models can be found in [12], whereas a sequential data fusion model in the field of complex numbers  $\mathbb{C}$  is introduced in [11]. One well established information fusion model is the so called waterfall model, shown in Figure 1.1. This framework comprises several stages of processing, starting from the raw data acquisition through to Situation Assessment and Decision Making stages. Notice that the Signal Processing, Feature Extraction, and Pattern Processing stages naturally belong to the area of signal processing.

By design, EMD has a natural ability to perform both signal conditioning (denoising) and feature extraction. We further show that EMD provides a uni-

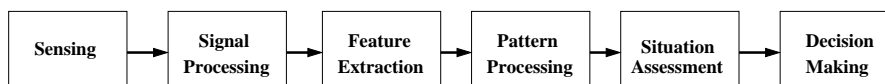


**Fig. 1.1.** The “waterfall model” of information fusion.

ifying framework for both the information *fission* (the phenomenon by which observed information is decomposed into a set its components) and *fusion*, whereby several stages from Figure 1.1, such as Signal Processing, Feature Extraction and Situation Assessment can be naturally performed by EMD. The Decision Making stage can be achieved based on EMD either by inspection or by post-processing in the form of some machine learning algorithm.

The aim of this work is therefore to provide theoretical and practical justification for the use of both real and complex EMD in knowledge extraction and information fusion. For convenience, this is achieved by an extension of the standard, real valued, EMD method to the field of complex numbers  $\mathbb{C}$ . The analysis is general and is supported by an extensive set of simulations on point processes, such as spike trains coming from networks of spiking neurons.

## 1.2 Empirical Mode Decomposition

Empirical mode decomposition [7] is a technique to adaptively decompose a given signal, by means of a process called the sifting algorithm, into a finite set of oscillatory components. These components, called “intrinsic mode functions” (IMFs), represent the oscillation modes embedded in the data. The IMFs act as a naturally derived set of basis functions for the signal; EMD can thus be seen as an exploratory data analysis technique. In fact, EMD and the Hilbert-Huang Transform comprise the so-called “Hilbert Spectral Analysis” [7]; a unique spectral analysis technique employing the concept of instantaneous frequency. In general, the EMD aims at representing an arbitrary signal via a number of IMFs and the residual. More precisely, for a real-valued signal  $x[k]$ , the EMD performs the mapping

$$x[k] = \sum_{i=1}^N c_i[k] + r[k] \quad (1.1)$$

where the  $c_i[k]$ ,  $i = 1, \dots, N$  denote the set of IMFs and  $r[k]$  is the trend within the data (also referred to as the last IMF or residual). By design, an IMF is a function which is characterized by the following two properties: the upper and lower envelope are symmetric; and the number of zero-crossings and the number of extrema are exactly equal or they differ at most by one.

In order to extract the IMFs from a real world signal, the *sifting* algorithm is employed, which is described in Table 1. Following the sifting process, the

**Table 1.1. The EMD algorithm**

1. Connect the local maxima of the signal with a spline. Let U denote the spline that forms the upper envelope of the signal;
2. Connect the local minima of the signal with a spline. Let L denote the spline that forms the lower envelope of the signal;
3. Subtract the mean envelope  $m = \frac{U+L}{2}$  from the signal to obtain a proto-IMF;
4. Repeat Steps 1, 2 and 3 above until the resulting signal is a proper IMF (as described above). The IMF requirements are checked indirectly by evaluating a stoppage criterion, originally proposed as:

$$\sum_{k=0}^T |h_{n-1}[k] - h_n[k]|^2 h_{n-1}^2[k] \leq SD \quad (1.2)$$

where  $h_n[k]$  and  $h_{n-1}[k]$  represent two successive sifting iterates. The SD value is usually set to 0.2 – 0.3;

5. After finding an IMF, this same IMF is subtracted from the signal. The residual is regarded as new data and fed back to Step 1 of the algorithm;
6. The algorithm is completed when the residual of Step 5 is a monotonic function. The last residual is considered to be the trend.

Hilbert Transform can be applied to each IMF separately. This way, it is possible to generate analytic signals, having an IMF as the real part and its Hilbert Transform as the imaginary part, that is  $x + j\mathcal{H}(x)$  where  $\mathcal{H}$  is the Hilbert Transform operator. Equation (1.1) can therefore be augmented to its analytic form given by

$$X(t) = \sum_{i=1}^n a_i(t) \cdot e^{j\theta_i(t)} \quad (1.3)$$

where the trend  $r(t)$  is purposely omitted, due to its overwhelming power and lack of oscillatory behavior. Observe from (1.3), that now the time dependent amplitude  $a_i(t)$  can be extracted directly and that we can also make use of the phase function  $\theta_i(t)$ . Furthermore, the quantity  $f_i(t) = \frac{d\theta_i}{dt}$  represents the instantaneous frequency [2]; this way by plotting the amplitude  $a_i(t)$  versus time  $t$  and frequency  $f_i(t)$ , we obtain a Time-Frequency-Amplitude representation of the entire signal called the Hilbert Spectrum. It is this combination of the concept of instantaneous frequency and EMD that makes the framework so powerful as a signal decomposition tool.

To illustrate the operation of EMD, consider a signal which consists of two added sinewaves with different frequencies, shown in Figure 1.2 (Left) (the original signal is in the first row, followed by the corresponding IMFs C1–C2, for convenience the last IMF is denoted by R3), and its Hilbert spectrum (Figure 1.2 (Right)). Observe the “fission” process performed by EMD,

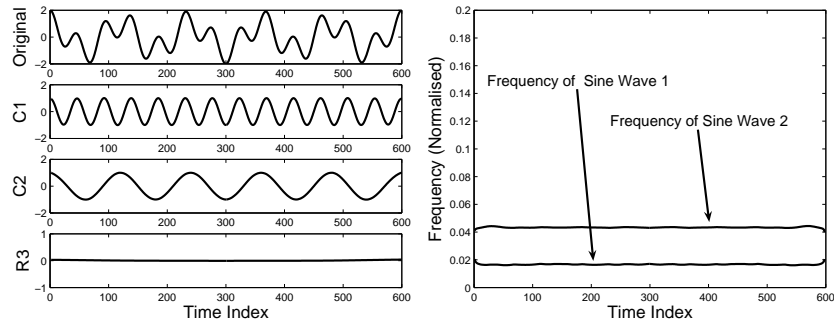


**Fig. 1.2.** EMD of two concatenated sinewaves. Left: Intrinsic mode functions; Right: Hilbert spectrum.

whereby the original signal is split into a set of IMFs (C1–C2) and residual (R3). The frequencies of the sine waves composing the original signal are clearly visible in the time–frequency spectrum (Figure 1.2 Right).

Another example of the usefulness of EMD in both the “Signal Processing” and “Feature Extraction” module from the “waterfall” information fusion model from Figure 1.1 is the so called blood volume estimation [14]. In

this application, a sensor in human heart records both the blood flow (near sinusoidal) and the superimposed Electro-Cardiogram (ECG). The goal is to extract pure blood volume signal, since this information is crucially important in heart surgery. This is also a very difficult signal processing problem since the ECG and blood volume are coupled and standard signal processing techniques (both supervised and blind) are bound to fail. By applying EMD to this problem, we were able to both denoise the useful blood volume signal (remove the ECG artifact) and to extract (by visual inspection) the IMFs which represent blood volume (IMFs C7–C9), as illustrated in Figure 1.3. This demonstrates the “fusion” via “fission” abilities of EMD.

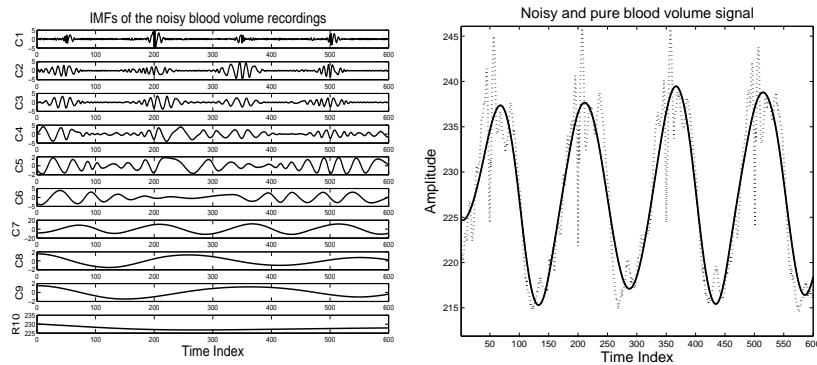


**Fig. 1.3.** EMD for *signal processing* (denoising) and *feature extraction* from coupled noisy blood volume recordings. Left: Intrinsic mode functions; Right: The original noisy blood volume signal (dotted line) and the extracted pure blood volume constructed by fusion of IMFs C7–C9 (solid line).

### 1.3 Ensemble Empirical Mode Decomposition (EEMD)

A drawback of EMD is the appearance of disparate scales across *different* IMF components, known as mode mixing. This is often the result of signal intermittancy and can leave the IMF components devoid of physical meaning. One answer to this problem is a noise-assisted data analysis (NADA) method called Ensemble EMD (EEMD) [6]. The EEMD defines the true IMF components as the mean of an ensemble of trials, each consisting of the signal corrupted by additive white noise of finite variance. The principle of the EEMD is simple: the added white noise populates the whole time-frequency space uniformly, facilitating a natural separation of the frequency scales that reduces the occurrence of mode mixing.

By an ensemble average, the effect of the added white noise with standard deviation  $\varepsilon$  decreases as

$$\varepsilon_n = \frac{\varepsilon}{\sqrt{N}} \Leftrightarrow \ln \varepsilon_n + \frac{\varepsilon}{2} \ln N = 0 \quad (1.4)$$

where  $N$  is the number of ensemble members, and  $\varepsilon_n$  is defined as the final standard deviation of for each ensemble member (a difference between the input signal and the sum of corresponding IMFs).

To illustrate the performance of EEMD, we consider a set of highly noisy recordings of brain neuronal activity obtained from a cortex implant (trains of spiking neurons). The dataset was obtained within the European Project Neuroprobes ([www.neuroprobes.org](http://www.neuroprobes.org)); the data were sampled at 44 kHz, and the Probe NP-PA-09 was used for which the impedance was 28.8 k $\Omega$ . The neuronal spikes were produced from the stimulation of the tongue of a monkey; although the spikes of neuronal activity were recorded, they could not be detected due to a very high background noise level. Figure 1.4 shows the recorded signals and the IMFs (C1-R8) produced by the EEMD algorithm; notice that spiky signals were detected in IMF C4 (due to the analogue amplifiers these spikes are somewhat integrated). The IMF of interest was then

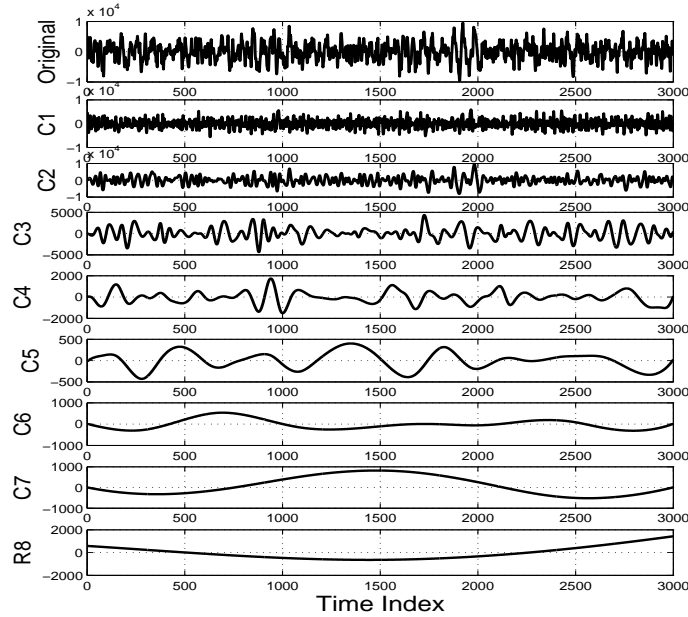


**Fig. 1.4.** Ensemble Empirical Mode Decomposition of recorded neuronal spikes.

compared with the originally recorded noisy signal in Fig. 1.5, clearly indicating the ability of EEMD to extract the signal of interest.

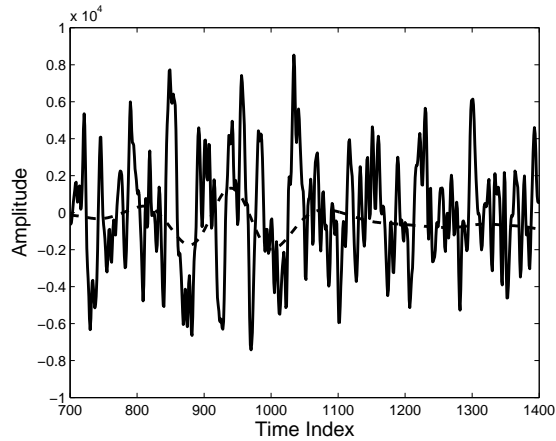


**Fig. 1.5.** The main component of the extracted brain neuronal recording, that is, IMF C4 from Figure 1.4 (thick dotted line) compared with the original noisy signal (solid line).

To further demonstrate the knowledge extraction abilities of EMD with real data, we consider its application in the removal of unwanted ocular artifacts (caused by eye activity of the subject) from electroencephalogram (EEG) data. The unwanted artifacts are a major obstacle for real-time brain computer interface (BCI) applications, since they occupy the low frequency range of EEG (0 - 13 Hz) and cannot be removed by conventional filtering methods due to overlapping of their respective spectra in a non stationary and nonlinear environment. In order to equip EMD to perform the *Decision Making* stage of the information fusion model (Figure 1.1), in the postprocessing stage we employed an adaptive filtering type machine learning algorithm which automatically combined the relevant IMFs to produce the signal with the artifact removed. This is verified on the EEG data obtained from the Fp1 electrode (placed close to the forehead); the original signal and several of the extracted IMFs are plotted in Figure 1.6. Note the inherent “fission”, that is, the original signal was decomposed into a number of its oscillating modes. An artifact-free reconstruction of the EEG signal (see Figure 1.7) was achieved by fusion of the relevant IMFs, that is the IMFs that correspond to instantaneous frequencies outside of the range dominated by the ocular artifacts [9]. The fusion process employed a block based approximation [18], based on minimization of the mean square error.

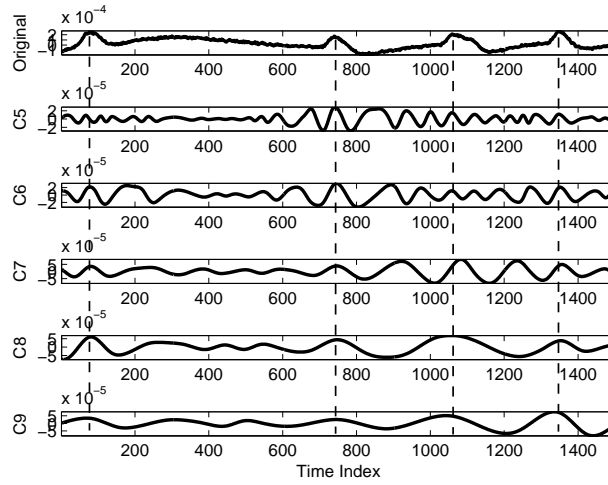


**Fig. 1.6.** The EEG signal, with blink artifacts at time instants 80, 740, 1070 and 1350, is displayed at the top of the Figure. Additional plots show some of the extracted IMFs. Note there is no discernable change in frequency surrounding peaks (denoted on the plots by the dashed line), but that the IMF components at the event of spike are in phase.

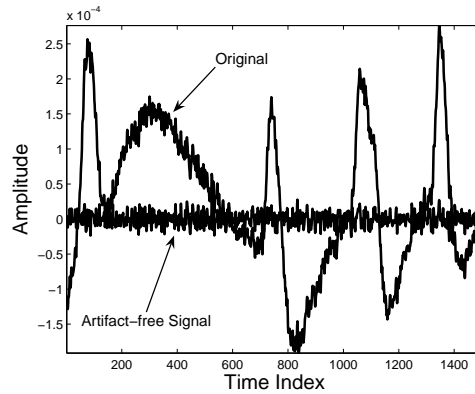


**Fig. 1.7.** Automated fusion of “relevant” IMFs to reconstruct artifact-free EEG signal (solid line).

We now investigate the singular problem of detecting the ocular peaks as they occur in the EEG signal. Consider again Figure 1.6 and the IMFs obtained in regions contaminated by an artifact. Since there is no discernable change in the frequencies of the IMFs surrounding artifact events, standard



Hilbert-Huang analysis will fail to detect the presence of the relatively significant change in the signal dynamics, a shortcoming of standard EMD signal analysis. After a visual inspection of the IMFs, it is clear that several of the IMF peaks coincide at the time instant of the artifact. In other words, the IMFs are in phase when the signal peak occurs. This example demonstrates that even in the case of real valued data, a rigorous analysis of phase (joint complex valued amplitude and phase) activity is necessary for complete analysis.

## 1.4 Extending EMD to the Complex Domain

Complex data is a bivariate quantity with a mutual dependence between the real and imaginary components. Additionally, arithmetic operations on  $\mathbb{C}$  form a unique algebra. Although an attractive solution might appear to be the application of real EMD to both the real and imaginary components separately, this mapping onto two independent univariate quantities will crucially ignore any mutual information that existed between the original components (phase). The same can be said, for example, of the separate application of EMD to the amplitude and phase functions of a complex data set. Furthermore, a critical aspect of EMD is that the IMFs have a physical interpretation.

We shall now examine the effectiveness of our two recently introduced extensions of EMD to the complex domain in the proposed framework. Each of the algorithms strive to retain capabilities and properties of real-valued EMD. The first method, termed “Complex Empirical Mode Decomposition”, is based on the direct use of the properties of the Hilbert Transform [15]. The second method, “Rotation Invariant Empirical Mode Decomposition”, is a generic extension of the real EMD [1].

### 1.4.1 Complex Empirical Mode Decomposition

The first method to “complexify” EMD was introduced in 2007, termed Complex Empirical Mode Decomposition [15]. The method is rigorously derived, based on the inherent relationship between the positive and negative frequency components of a complex signal and the properties of the Hilbert Transform. The idea behind this approach is rather intuitive: first note that a complex signal has a two-sided, asymmetric spectrum. The complex signal can therefore be converted into a sum of analytic signals by a straightforward filtering operation that extracts the opposite sides of the spectrum. Direct analysis in  $\mathbb{C}$  can subsequently be achieved by applying standard EMD to both the positive and negative frequency parts of the signal. Given a complex signal  $x[k]$ , real valued components corresponding to the positive and negative sides of the spectrum can be extracted as

$$\begin{aligned} x_+[k] &= \mathcal{RF}^{-1} \{X(e^{j\omega}) \cdot H(e^{j\omega})\} \\ x_-[k] &= \mathcal{RF}^{-1} \{X(e^{j\omega}) \cdot H(e^{-j\omega})\} \end{aligned} \quad (1.5)$$

where  $\mathcal{F}^{-1}$  is the inverse Fourier Transform,  $\mathcal{R}$  is an operator that extracts the real part of a signal, and  $H(e^{j\omega})$  is an ideal filter with the transfer function

$$H(e^{j\omega}) = \begin{cases} 1, & \omega > 0 \\ 0, & \omega < 0 \end{cases}$$

Given that  $x_+[k]$  and  $x_-[k]$  are real valued, standard EMD can be applied to obtain a set of IMFs for each analytic signal. This can be expressed as

$$\begin{aligned} x_+[k] &= \sum_{i=1}^{N_+} x_i[k] + r_+[k] \\ x_-[k] &= \sum_{i=-N_-}^{-1} x_i[k] + r_-[k] \end{aligned} \quad (1.6)$$

where  $\{x_i[k]\}_{i=1}^{N_+}$  and  $\{x_i[k]\}_{i=-N_-}^{-1}$  denote sets of IMFs corresponding, respectively to  $x_+[k]$  and  $x_-[k]$ , whereas  $r_+[k]$  and  $r_-[k]$  are the respective residuals. The original complex signal can be reconstructed by

$$x[k] = (x_+[k] + j\mathcal{H}[x_+[k]]) + (x_-[k] + j\mathcal{H}[x_-[k]])^* \quad (1.7)$$

where  $\mathcal{H}$  is the Hilbert transform operator. To conclude the derivation, a single set of complex IMFs corresponding to the complex signal  $x[k]$  is given by

$$x[k] = \sum_{i=N_-, i \neq 0}^{N_+} y_i[k] + r[k] \quad (1.8)$$

where  $r[k]$  is the residual and  $y_i[k]$  is defined by

$$y_i[k] = \begin{cases} (x_+[k] + j\mathcal{H}[x_+[k]]), & i = 1, \dots, N_+, \\ (x_-[k] + j\mathcal{H}[x_-[k]])^*, & i = -N_-, \dots, -1 \end{cases}$$

To illustrate this technique, consider a problem involving real world data of several streams: neuronal spike modelling in BCI. The task is to detect any synchronisation that occurs between spiking neuron time series. For our simulations, two spiking neuron time series (see Figure 1.8) were generated using the tool described in [13]. The simulation time was set to 0.2 seconds and the sampling frequency to 10 KHz. We note that there are synchronised spikes at time instants 750, 1350 and  $1800 \times 10^{-1}$  ms.

Although the two time series ( $x_1[k]$  and  $x_2[k]$ ) are real-valued, a complex signal,  $z[k] = x_1[k] + jx_2[k]$ , is constructed with the signals representing the real and imaginary parts respectively. The IMFs and the Hilbert spectra corresponding to the positive and the negative frequency parts of the signal  $z[k]$  are shown respectively in Figures 1.9 and 1.10. Observe that complex EMD has failed to reveal any synchronised events between the data streams. To its

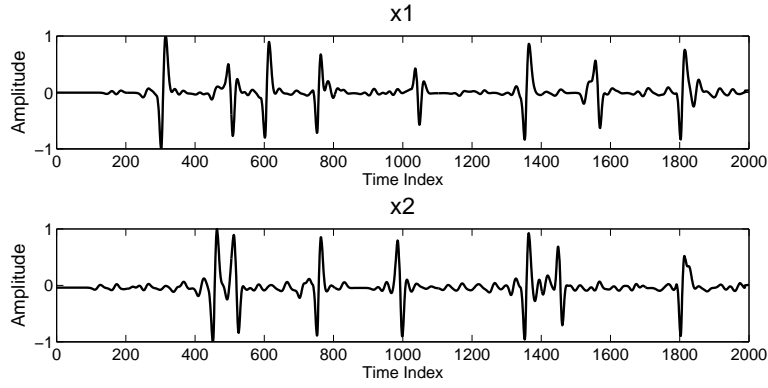


**Fig. 1.8.** Point processes  $x_1$  and  $x_2$ , note the synchronised spikes at time instants  $750, 1350$  and  $1800 \times 10^{-1}$  ms.

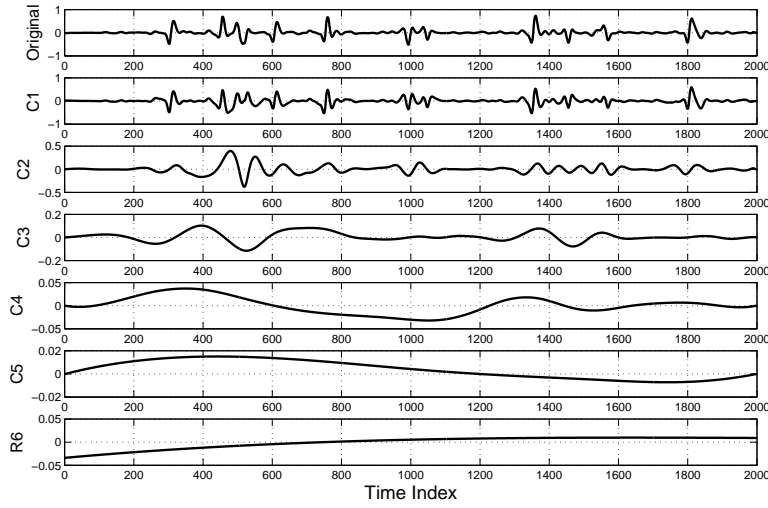


**Fig. 1.9.** IMFs corresponding to the positive frequencies of the signal  $z[k] = x_1[k] + jx_2[k]$ .

advantage though, it has a straightforward, intuitive mathematical derivation. As an example of its mathematical robustness, it preserves the dyadic filter property of standard EMD. In other words, the algorithm acts as dyadic filter bank when processing complex noise [15].

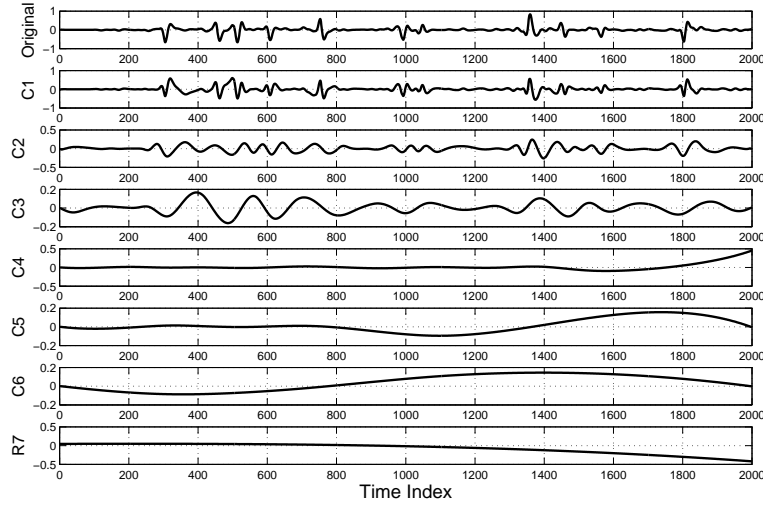


**Fig. 1.10.** The IMFs corresponding to the negative frequencies of the signal  $z[k] = x_1[k] + jx_2[k]$ , note that compared to Figure 1.10 there are a different number of IMFs.

It is in fact the precise mathematical derivation that deprives the resulting IMFs of their physical connection with the original data set. This is demonstrated by observing Figures 1.9 and 1.10 and noting that the number of IMFs obtained from the positive and negative part of the complex signal  $z[k]$  are different. Another disadvantage is the ambiguity at zero frequency, a problem inherited from the properties of the Hilbert Transform. Furthermore, the method cannot be extended to higher dimensions due to the limitation of representing a signal by its positive and negative frequencies. It should be finally noted that the mean should be removed before applying complex EMD as the Hilbert Transform ignores constants.

$$\mathcal{H}\{x[k] + c\} = \mathcal{H}\{x[k]\} \quad (1.9)$$

where  $\mathcal{H}$  is the Hilbert Transform operator.

#### 1.4.2 Rotation Invariant Empirical Mode Decomposition

Rotation Invariant EMD, introduced in [1], proposes a way of extending EMD theory so that it operates fully in  $\mathbb{C}$ . This is achieved through the use of complex splines. Unlike Complex EMD, by design this method generates an equal number of IMFs for the real and imaginary parts; these can be given physical meaning thus retaining an important property of real valued EMD. A critical

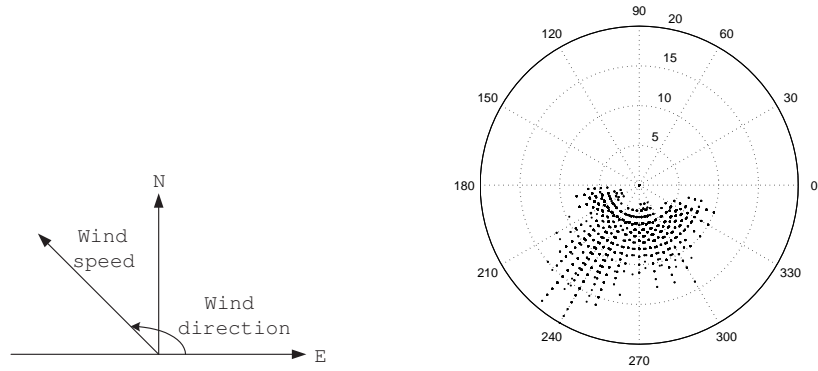


**Fig. 1.11.** Wind as a complex vector field. Left: a complex vector of wind speed  $v$  and direction  $d$  ( $ve^{jd}$ ); Right: the wind lattice [4], a set of complex valued wind data.

aspect of the derivation of EMD in  $\mathbb{C}$  is the definition of an extremum. Several possible approaches are suggested in [1] such as the extrema of the modulus and the locus where the angle of the first order derivative (with respect to time) changes sign; this way it can be assumed that a local maxima will be followed by a local minima (and vice versa). This definition is equivalent to the extrema of the imaginary part, that is, for a complex signal  $Z(t)$  (for convenience we here use a continuous time index  $t$ )

$$\begin{aligned} \angle \dot{Z}(t) = 0 &\Rightarrow \angle \{\dot{x}(t) + j \cdot \dot{y}(t)\} = 0 \\ &\Rightarrow \tan^{-1} \frac{\dot{y}(t)}{\dot{x}(t)} = 0 \Rightarrow \dot{y}(t) = 0 \end{aligned} \quad (1.10)$$

To illustrate the Rotation Invariant EMD, consider a set of wind<sup>1</sup> speed and direction measurements, which have been made complex, as illustrated in Figure 1.11. The problem of the choice of the criterion for the extrema of the complex function and one IMF generated by the Rotation Invariant EMD are shown in Figure 1.12. Clearly, the choice of criterion for finding the extrema of a complex signal is not unique, the extracted complex IMFs however do possess physical meaning; consider IMF 6 from Figure 1.12 which reflects the level of detail for a given time-scale.

### 1.4.3 Complex EMD as Knowledge Extraction Tool for Brain Prosthetics

Consider again the complex signal  $z[k] = x_1[k] + jx_2[k]$  from the previous section, constructed from the two real-valued spiking neuron time series. The task is to detect the event of spike synchronisation, that is when the two

<sup>1</sup> Publicly available from <http://mesonet.agron.iastate.edu/request/awos/1min.php>

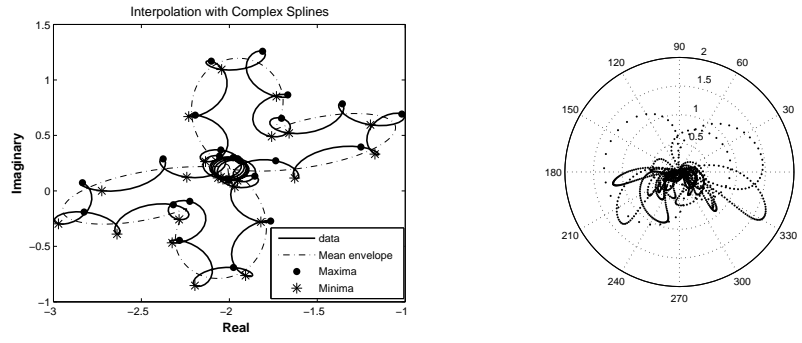


**Fig. 1.12.** Wind field analysed by the Rotation Invariant Complex EMD. Left: the original complex signal and the extrema; Right: IMF 6 extracted from the wind data.

neurons fire simultaneously. Rotation invariant EMD allows us to achieve this, due to the equal number of IMFs for the real and imaginary part of  $z[k]$ , as shown in Figures 1.13 and 1.14, showing respectively IMFs obtained using the “extrema of the modulus” and “zero-crossings of the angle of the first derivative” criteria. By design, two spiking events will be synchronised

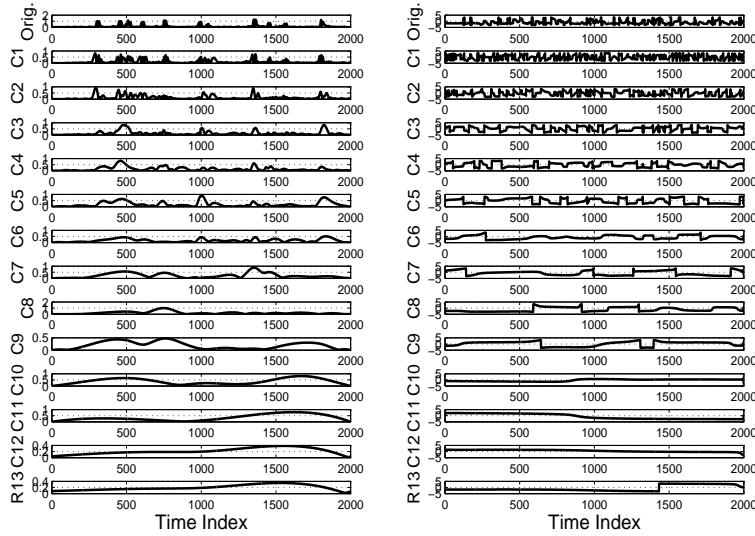


**Fig. 1.13.** Magnitude and phase of IMFs determined by rotation invariant EMD. Criterion: extrema of the modulus.

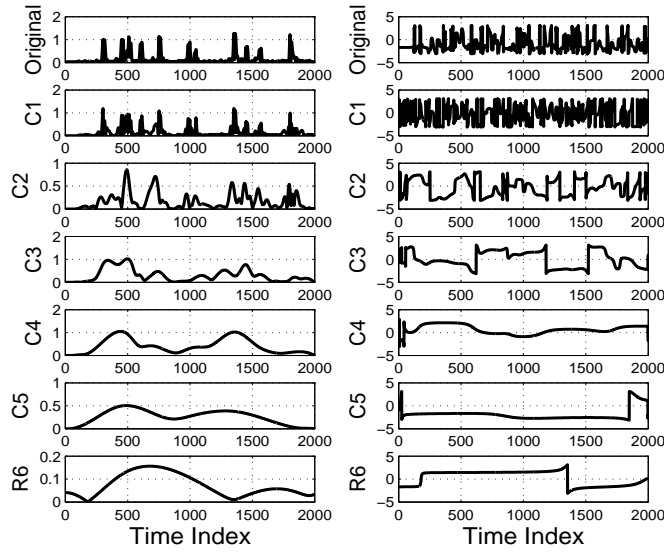


**Fig. 1.14.** Magnitude and phase of IMFs determined by rotation invariant EMD. Criterion: zero crossings of the angle of the first derivative. This criterion is equivalent to finding the extrema of the imaginary part; the corresponding IMFs are identical.

if the phase of  $z[k]$  is  $\frac{\pi}{4}$ . Since the spikes are high frequency events, most of the relevant information is contained in the first few IMFs. To illustrate the detection of synchronised spikes, consider the first IMF obtained by the “modulus” criterion (top of Figure 1.13). The magnitude and phase of this first IMF is given in Figure 1.15. Note that large peaks in the magnitude of the first IMF do not exclusively indicate synchronisation of the spikes, however, from the phase obtained we can easily distinguish between arbitrary maxima events and synchronisation events. From Figure 1.15, as desired, all synchronised spiking events occur at the same phase of  $\frac{\pi}{4}$  (denoted by the iso-phase line).

### 1.5 Empirical Mode Decomposition as a Fixed Point Iteration

The sifting process within EMD can be viewed as iterative application of a nonlinear operator  $T$  on a signal. The action of the operator can be described by:

$$T[h_k] = h_{k+1} = h_k - m_k(h_k) \tag{1.11}$$

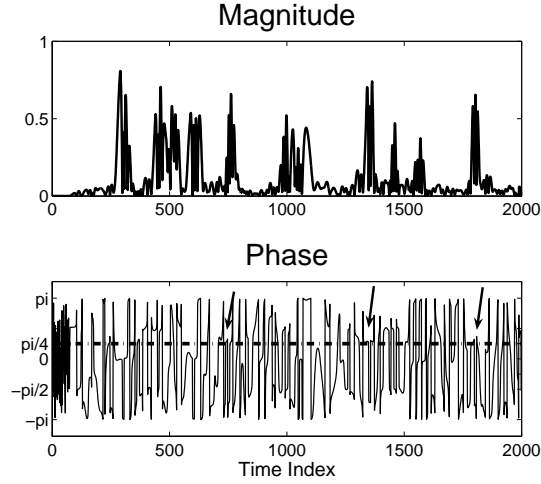


**Fig. 1.15.** The magnitude and phase of the first IMF extracted with the modulus criterion can be used to detect spike synchronization.

where  $h_k$  denotes the result of the  $k^{\text{th}}$  iteration and  $m_k$  is the  $k^{\text{th}}$  local mean signal (depending on  $h_k$ ). From their definition, IMFs have a zero local mean, therefore, for an extracted IMF, equation (1.11) becomes:

$$T[h_k] = h_k \quad (1.12)$$

indicating that IMFs can be viewed as fixed points of the iteration  $h_{k+1} = T[h_k]$ .

Theoretically, the iteration (1.11) could converge in only one step. However since the true local mean is unknown, a spline approximation is used. Indeed, the existence of hidden scales, can result in the appearance of new extrema after every round of sifting. For these reasons, sifting is carried out several times, until the stoppage requirement (e.g. (1.2)) is satisfied. Practically, sifting to the extreme would remove all the amplitude modulation and would result in purely frequency modulated components (IMFs). This is not desired because this drains the physical meaning from the IMFs [7].

To summarise, from the series of approximations (see Table 1.1):

$$h_1, h_2, \dots, h_k, \dots, h_\infty \quad (1.13)$$

EMD picks up at each iteration a term that retains enough variation according to the predefined stoppage criterion. A slight modification of the stoppage criterion to a symmetric one such as:

$$d_1(h_k, h_{k-1}) = \sum_{t=0}^T \frac{|h_{k-1}(t) - h_k(t)|^2}{T} \quad (1.14)$$



or

$$d_2(h_k, h_{k-1}) = \sum_{t=0}^T \frac{|h_{k-1}(t) - h_k(t)|^2}{|h_{k-1}(t) + h_k(t)|^2} \quad (1.15)$$

would immediately turn the stoppage criterion into a metric, as desired (by the Contraction Mapping Theorem (CMT) [10]. In combination with an analytic expression for the mean value of the signal such as the one proposed in [3], this would lead to the verification of the Lipschitz continuity of the series (1.13). The Lipschitz continuity can be used to determine:

1. The existence of IMFs, via convergence of (1.13), through application of the Contraction Mapping Theorem [8] or;
2. Uniqueness and conditions on the class of signals for which the series converges;
3. The speed of convergence.

## 1.6 Discussion and Conclusions

The concept of multichannel information fusion via the inherent fission abilities of standard Empirical Mode Decomposition (EMD) has been introduced. This is achieved by starting from standard real EMD and extending it to the fusion of data in higher dimensions. It has been shown that even for real valued data, their processing in the field of complex numbers  $\mathbb{C}$  offers great advantages, for instance when the phase information is important. Both real and complex EMD have been shown to provide a unified approach to information fusion via fission, naturally performing data processing (denoising) and feature extraction. In addition, it has been illustrated that EMD also provides the decision stage within the information fusion framework. This can be achieved either by inspection or by intelligent fusion of Intrinsic Mode Functions (IMFs) through a suitable machine learning algorithm. The IMFs obtained from the Rotation Invariant EMD have been shown to have physical meaning, which greatly enhances the range of applications of this technique. A rigorous theoretical framework for the analysis of EMD using the Fixed Point Theory (FPT) methodology has also been addressed.

The simulations have been conducted on real world problems in Brain Computer Interface (BCI), including eye blink artifact removal from Electro-Encephalograms (EEG), and spike detection and synchronisation for brain prosthetics based on an array of implanted electrodes in the surface of the brain cortex.

## Acknowledgements

The authors acknowledge support from the NeuroProbes project, 6th framework programme of the European Commission (IST-2004-027017).

## References

1. Altaf, M.U.B., Gautama, T., Tanaka, T., Mandic, D.P.: Rotation invariant complex empirical mode decomposition. In: Proceedings of the International Conference on Acoustics, Speech and Signal Processing (ICASSP), vol. 3, pp. 1009–1012 (2007)
2. Cohen, L.: Instantaneous anything. In: Proceedings of the IEEE International Conference on Acoustics, Speech and Signal Processing (ICASSP), vol. 5, pp. 105–108 (1993)
3. Delechelle, E., Lemoine, J., Niang, O.: Empirical mode decomposition: An analytical approach for sifting process. *IEEE Signal Processing Letters* **12**, 764 – 767 (2005)
4. Goh, S.L., Chen, M., Popovic, D.H., Aihara, K., Obradovic, D., Mandic, D.P.: Complex-valued forecasting of wind profile. *Renewable Energy* **31**(1733–1750), tba (2006)
5. Hall, D.L., Llinas, J.: An introduction to multisensor data fusion. *Proceedings of the IEEE* **85**(1), 6–23 (1997)
6. Hu, J., Yang, Y.D., Kihara, D.: EMD: an ensemble algorithm for discovering regulatory motifs in DNA sequences. *BMC Bioinformatics* **7**, 342 (2006)
7. Huang, N.E., Shen, Z., Long, S.R., Wu, M.L., Shih, H.H., Quanan, Z., Yen, N.C., Tung, C.C., Liu, H.H.: The empirical mode decomposition and the Hilbert spectrum for nonlinear and non-stationary time series analysis. *Proceedings of the Royal Society A* **454**, 903–995 (1998)
8. Leibovic, K.N.: Contraction mapping with application to control processes. *Journal of Electronics and Control* pp. 81–95 (1963)
9. Looney, D., Li, L., Rutkowski, T.M., Mandic, D.P., Cichocki, A.: Ocular artifacts removal from eeg using emd. In: Proceedings of the 1st International Conference on Cognitive Neurodynamics (ICCN) (2007)
10. Mandic, D.P., Chambers, J.A.: *Recurrent Neural Networks for Prediction: Architectures, Learning Algorithms and Stability*. Wiley (2001)
11. Mandic, D.P., Goh, S.L., Aihara, K.: Sequential data fusion via vector spaces: Fusion of heterogeneous data in the complex domain. *International Journal of VLSI Signal Processing Systems* **48**(1–2), 98–108 (2007)
12. Mandic, D.P., Obradovic, D., Kuh, A., Adali, T., Trutschell, U., Golz, M., Wilde, P.D., Barria, J., Constantinides, A., Chambers, J.: Data fusion for modern engineering applications: An overview. In: Proceedings of the IEEE International Conference on Artificial Neural Networks (ICANN'05), pp. 715–721 (2005)
13. Smith, L.S., Mtetwa, N.: A tool for synthesizing spike trains with realistic interference. *Journal of Neuroscience Methods* **159**(1), 170–180 (2006)
14. Souretis, G., Mandic, D.P., Griselli, M., Tanaka, T., Hulle, M.M.V.: Blood volume signal analysis with empirical mode decomposition. In: Proceedings of the 15th International DSP Conference, pp. 147–150 (2007)
15. Tanaka, T., Mandic, D.P.: Complex empirical mode decomposition. *IEEE Signal Processing Letters* **14**(2), 101–104 (Feb 2007)
16. Wald, L.: Some terms of reference in data fusion. *IEEE Transactions on Geosciences and Remote Sensing* **37**(3), 1190–1193 (1999)
17. Waltz, E., Llinas, J.: *Multisensor Data Fusion*. Artech House (1990)
18. Weng, B., Barner, K.E.: Optimal and bidirectional optimal empirical mode decomposition. In: Proceedings of the International Conference on Acoustics, Speech and Signal Processing (ICASSP), vol. 3, pp. 1501–1504 (2007)

---

## Index

- Data fusion
  - data fusion via fission, 4, 7
  - waterfall model, 2
- Electroencephalogram, EEG
  - ocular artifacts, 7
- Empirical mode decomposition, 3
  - complex EMD, 9
  - ensemble EMD, 5
- fixed point iteration, 15
- rotation invariant EMD, 12
- sifting algorithm, 3
- Neuronal spikes, 6, 10, 13
- Wind modelling
  - complex EMD, 13